MICROSCOPIC PHASE SEPARATION AND TWO TYPES OF QUASIPARTICLES IN LIGHTLY DOPED $La_{2-x}Sr_xCuO_4$ OBSERVED BY ELECTRON PARAMAGNETIC RESONANCE

A. Shengelaya[1] , *M. Bruun*[1], *K.A. Müller*[1], *A. Safina*[2], *K. Conder*[3]

[1] Physik-Institut der Universität Zürich, Zürich CH-8057, Switzerland
[2] Kazan State University, Kazan, 420008, Russia
[3] ETH Zürich and PSI, CH-5232 Villigen PSI, Switzerland

МИКРОСКОПИЧЕСКОЕ ФАЗОВОЕ РАССЛОЕНИЕ И ДВА ТИПА КВАЗИЧАСТИЦ, ОБНАРУЖЕННЫЕ МЕТОДОМ ЭЛЕКТРОННОГО ПАРАМАГНИТНОГО РЕЗОНАНСА В СЛАБО ДОПИРОВАННОМ $La_{2-x}Sr_xCuO_4$

А. Шенгелая[1], *М. Бруун*[1], *К.А. Мюллер*[1], *А. Сафина*[2], *К. Цондер*[3]

[1] Цюрихский университет, Цюрих, Швейцария
[2] Казанский государственный университет, Казань
[3] Высшая техническая школа, Виллиген, Швейцария

Magnetic Resonance in Solids
Electronic Journal

Volume **6**, *No.* **1**,
pages **191-197**, **2004**

http://mrsej.ksu.ru

MICROSCOPIC PHASE SEPARATION AND TWO TYPES OF QUASIPARTICLES IN LIGHTLY DOPED $La_{2-x}Sr_xCuO_4$ OBSERVED BY ELECTRON PARAMAGNETIC RESONANCE

A. Shengelaya[1], M. Bruun[1], K.A. Müller[1], A. Safina[2], K. Conder[3]
[1] *Physik-Institut der Universität Zürich, Zürich CH-8057, Switzerland*
[2] *Kazan State University, Kazan, 420008, Russia*
[3] *ETH Zürich and PSI, CH-5232 Villigen PSI, Switzerland*

In the low doping range of x from 0.01 to 0.06 in $La_{2-x}Sr_xCuO_4$, we observed two electron paramagnetic resonance (EPR) signals: a narrow and a broad one. The narrow line is ascribed to metallic regions in the material, and its intensity increases exponentially upon cooling below ~ 150 K. The activation energy deduced $\Delta = 460(50)$ K is nearly the same as that found in the doped superconducting regime by Raman and neutron scattering. Obtained results provide evidence of the microscopic phase separation and two type of quasiparticles in lightly doped $La_{2x}Sr_xCuO_4$.

The mechanism of high-T_c superconductivity (HTSC) remains enigmatic even after 17 years of its discovery [1]. It is known that HTSC is achieved when a moderate density of conducting holes is introduced in the CuO_2 planes. At a critical concentration of doping $x_{cr} \approx 0.06$, superconductivity appears. However, it is still an unresolved issue how the electronic structure evolves with hole doping from the antiferromagnetic insulator to the paramagnetic metalllic and superconducting state. While most of the theoretical models assume that the holes are homogeneously doped into CuO_2 planes, there are increasing number of the experiments pointing towards highly nonuniform hole distribution leading to a formation of hole-rich and hole-poor regions [2]. This electronic phase separation is expected to be mostly pronounced at low hole concentrations. In the early experiments Johnston *et al.* analyzed the susceptibility of the $La_{2-x}Sr_xCuO_4$ (LSCO) samples at concentrations $x < x_{cr}$ using the finite-size scaling and concluded that the material consists of antiferromagnetic (AF) domains of variable size, separated by metallic domain walls [3]. More recently Ando *et al.* corroborated this early finding by measuring the in-plane resistivity anisotropy in untwinned single crystals of $La_{2-x}Sr_xCuO_4$ (LSCO) and $YBa_2Cu_3O_{7-\delta}$(YBCO) in the lightly doped region, interpreting their results in terms of metallic stripes present [4]. Furthermore, most recently, magnetic axis rotation was reported, and points to a high mobility of the crystallographic (metallic) domain boudaries of the AFM domains [5]. The Coulomb interaction limits the spatial extention of the electronic phase separation to hole-rich and hole-poor regions to a microscopic scale [6]. Therefore it is important to use a local microscopic methods to study the electronic phase separation in cuprates.

The nuclear magnetic resonance (NMR) is one of such methods. However, in lightly doped cuprates with $x < x_{cr}$ the NMR signal from Cu wipes out due to the strong AF fluctuations and no NMR signal can be observed at low temperatures [7]. On the other hand an electron paramagnetic resonance (EPR) signal can still be observed because the time-domain of observation of EPR is two to three orders of magnitude shorter than that of NMR [8]. In order to observe an EPR signal we doped LSCO with 2% of Mn, which in the 2+ valent state gives a well defined signal and substitutes for the Cu^{2+} in the CuO_2 plane. It was shown by Kochelaev *et al*. that the Mn ions are strongly coupled to the collective motion of the Cu spins (the so called bottleneck regime) [9]. Recently we have studied the EPR of Mn^{2+} in $La_{2-x}Sr_xCuO_4$ in a doping range $0.06 < x < 0.20$ [8]. The bottleneck regime allowed to obtain substantial information on the dynamics of the copper electron spins in the CuO_2 plane as a function of Sr doping and oxygen isotope substitution. In the present work we performed a thorough EPR investigation of the LSCO in lightly doped range $0.01 < x < 0.06$, i.e. below x_{cr}.

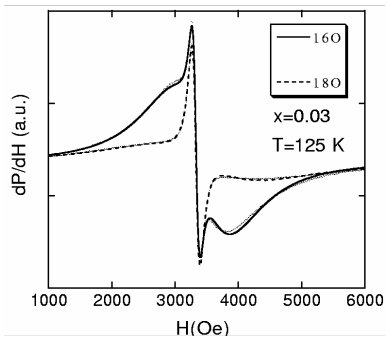

Fig.1. EPR signal of ^{16}O and ^{18}O samples of $La_{1.97}Sr_{0.03}Cu_{0.98}Mn_{0.02}O_4$ measured at T = 125 K under identical experimental conditions. The solid and dashed lines represent the best fits using a sum of two Lorentzian components with different linewidths: a narrow and a broad one

The $La_{2-x}Sr_xCu_{0.98}Mn_{0.02}O_4$ polycrystalline samples with $0 < x < 0.06$ were prepared by the standard solid-state reaction method. The EPR measurements were performed at 9.4 GHz using a BRUKER ER-200D spectrometer equipped with an Oxford Instruments helium flow cryostat. In order to avoid a signal distortion due to skin effects, the samples were ground and the powder was suspended in paraffin. We observed an EPR signal in all samples. The signal is centered near $g \sim 2$, a value very close to the g-factor for the Mn^{2+} ion.

Fig. 1 shows the EPR lines observed in $x = 0.03$ sample with different oxygen isotopes ^{16}O and ^{18}O. First, one should note that the EPR spectra consist of two lines. We found that they can be well fitted by a sum of two Lorentzian components with different linewidths: a narrow and a broad one. The second important observation is that the narrow line shows practically no isotope effect, whereas the broad line exhibits a huge isotope effect. Similar two-component EPR spectra were observed in other samples with different Sr concentrations up to $x = 0.06$. At $x = 0.06$, only a single EPR line is seen in the entire temperature range, in agreement with our previous studies of samples with $0.06 < x < 0.20$ [8].

Fig. 2 shows the temperature dependence of the EPR intensity for samples with different Sr concentrations. One can see that the two EPR lines follow a completely different temperature dependence. The intensity of the broad line has a maximum and strongly decreases with decreasing temperature. On the other hand, the intensity of the narrow line is negligible at high temperatures and starts to increase almost exponentially below ~150 K. We note that the temperature below which the intensity of the broad line decreases shifts to lower temperatures with increasing doping. However, the shape of the $I(T)$ dependence for the *narrow line is practically doping-independent* and only slightly shifts towards higher temperatures with increased doping. A similar

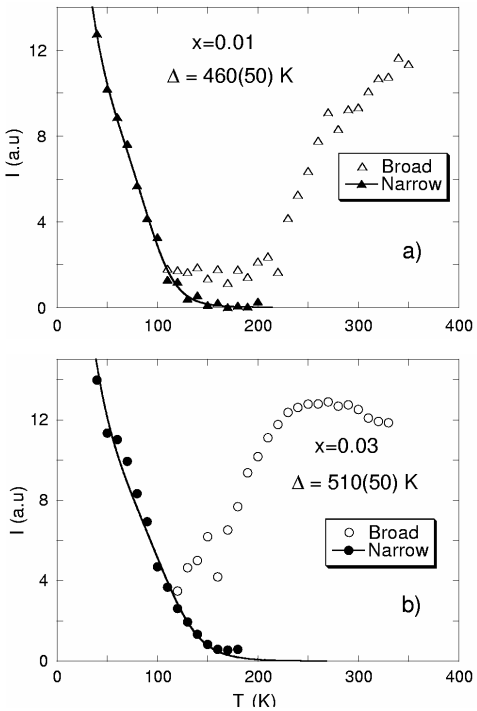

Fig.2.Temperature dependence of the narrow and broad EPR signal intensity in $La_{2x}Sr_xCu_{0.98}Mn_{0.02}O_4$ with different Sr dopings: ***(a)*** *$x = 0.01$;* ***(b)*** *$x = 0.03$. The solid lines represent fits using the model described in the text*

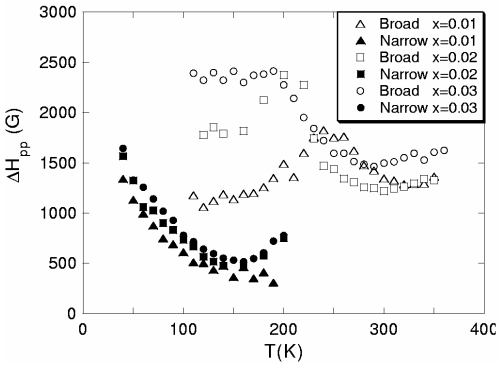

Fig. 3. Temperature dependence of the peak-to-peak linewidth ΔH_{pp} for the narrow and broad EPR lines in $La_{2-x}Sr_xCu_{0.98}Mn_{0.02}O_4$ with x = 0.01, 0.02 and 0.03

tendency is observed also for the temperature dependence of the EPR linewidth. The linewidth of the broad line and its temperature dependence are strongly doping-dependent, whereas the linewidth of the narrow line is very similar for samples with different Sr doping (see Fig. 3).

It is important to point out that the observed two-component EPR spectra are an intrinsic property of the lightly doped LSCO and are not due to conventional chemical phase separation. We examined our samples using *x*-ray diffraction, and detected no impurity phases. Moreover, the temperature dependence of the relative intensities of the two EPR signals rules out macroscopic inhomogeneities and points towards a microscopic electronic phase separation. The qualitatively different behavior of the broad and narrow EPR signals indicates that they belong to distinct regions in the sample. First we notice that the broad line vanishes at low temperatures. This can be explained by taking into account the AF order present in samples with very low Sr concentration [3]. It is expected that upon approaching the AF ordering temperature, a strong shift of the resonance frequency and an increase of the relaxation rate of the Cu spin system will occur. This will break the bottleneck regime of the Mn^{2+} ions, and as a consequence the EPR signal becomes unobservable [8].

In contrast to the broad line, the narrow signal appears at low temperatures and its intensity increases with decreasing temperature. This indicates that the narrow signal is due to the regions where the AF order is supressed. It is known that the AF order is destroyed by the doped holes, and above $x = 0.06$ AF fluctuations are much less pronounced [10]. Therefore, it is natural to relate the narrow line to regions with locally high carrier concentration and high mobility. This assumption is strongly supported by the absence of an oxygen isotope effect on the linewidth of the narrow line as well. It was shown previously that the isotope effect on the linewidth decreases at high charge-carrier concentrations close to the optimum doping [8]. We obtain another important indication from the temperature dependence of the EPR intensity. Because we relate the narrow line to hole-rich regions, an exponential increase of its intensity at low temperatures indicates an energy gap for the existence of these regions. In the following we will argue that this phase separation is assisted by the electron-phonon coupling. More precisely, the latter induces anisotropic interactions between the holes via the phonon exchange, resulting in the creation of extended nano-scale hole-rich regions.

An interaction between holes via the phonon exchange can be written in the form [11]:

$$H_{\text{hol-phon}} = G\sum_{n\alpha} P^{+}_{n\alpha}P_{n\alpha}\varepsilon_{\alpha\alpha}\,, \tag{1}$$

where $P_{n\alpha}{}^{+}$ is a creation operator of one polaron, $\varepsilon_{\alpha\alpha}$ is a deformation tensor, G is a coupling constant. It was shown that this interaction reduces to usual elastic forces if we neglect the retardation effects and optical modes. Following Aminov and Kochelaev [11], Orbach and Tachiki [12], we can find an interaction due to an exchange by phonons between two holes oriented along the axes α and β and separated by the space vector $\mathbf{R} = \mathbf{R}_{n\alpha} - \mathbf{R}_{m\beta}$

$$H = F(\mathbf{R}_{n\alpha} - \mathbf{R}_{m\beta})P^{+}_{n\alpha}P_{n\alpha}P^{+}_{m\beta}P_{m\beta}\,; \tag{2}$$

$$F_{xx}(\mathbf{R}) = \frac{1}{8\pi\rho C_l^2}\frac{G^2}{R^3}[2(1\text{-}3\gamma_x^2) + \eta(12\gamma_x^2\text{-}15\gamma_x^4\text{-}1)]\,, \tag{3}$$

$$F_{xy}(\mathbf{R}) = \frac{1}{8\pi\rho C_l^2}\frac{G^2}{R^3}(2\text{-}15\gamma_x^2\gamma_y^2)\,. \tag{4}$$

Here C_l, C_t are longitudinal and transversal sound velocities; $\gamma_x = x/R$, $\gamma_y = y/R$; $\eta = (C_l^2 - C_t^2)/C_t^2$. This interaction is highly anisotropic being attractive for some orientations and repulsive for others [13]. The attraction between holes may result in a bipolaron formation when holes approach each other closely enough. The bipolaron formation can be a starting point for the creation of hole-rich regions by attracting of additional holes. Because of the highly anisotropic elastic forces these regions are expected to have the form of stripes. Therefore the bipolaron formation energy Δ can be considered as an energy gap for the formation of hole-rich regions.

In applying the above model to the interpretation of our EPR results we have to keep in mind that the spin dynamics of the coupled Mn-Cu system experiences a strong bottleneck regime [9]. In the bottleneck regime the collective motion of the total magnetic moment of the Mn and Cu spin system appears because the relaxation rate between the magnetic moments of the Mn and Cu ions due to the strong isotropic Mn-Cu exchange interaction is much faster then their relaxation rates to the lattice. The intensity of the joint EPR signal, being proportional to the sum of spin susceptibilities $I \sim \chi_{\text{Mn}} + \chi_{\text{Cu}}$, is determined mainly by the Mn susceptibility, since $\chi_{\text{Mn}} \gg \chi_{\text{Cu}}$ for our Mn concentration and temperature range. This results in a Curie-Weiss temperature dependence of the EPR signal.

Taking into account this remark we conclude that the EPR intensity of the narrow line is proportional to the volume of the sample occuppied by the hole-rich regions because the Mn ions are randomly distributed in the sample. We expect that the volume in question is proportional to the number of bipolarons, which can be estimated in a way

proposed by Mihailovic and Kabanov [14]. If the density of states is determined *by* $N(E) \sim E^{\alpha}$, the number of bipolarons is

$$N_{\text{bipol}} = \left(\sqrt{z^2 + x} - z\right)^2, \quad z = KT^{\alpha+1} \exp\left(-\frac{\Delta}{T}\right), \tag{5}$$

where Δ is the bipolaron formation energy, x is the level of hole doping, and K is a temperature- and doping-independent parameter related to the free polaron density of states. The EPR intensity from the hole-rich regions will be proportional to the product of the Curie-Weiss susceptibility of the bottlenecked Mn-Cu system and the number of the bipolarons

$$I_{\text{narrow}} \sim \frac{C}{T-\theta} N_{\text{bipol}}, \tag{6}$$

where C is the Curie constant and θ is the Curie-Weiss temperature. The experimental points for the narrow-line intensity were fitted for the two-dimensional system ($\alpha = 0$), and we used the value $\theta = -8$ K, which was found from measurements of the static magnetic susuceptibility (an attempt to vary θ yielded about the same value). The values of C and θ are determined mainly by the concentration and magnetic moment of the Mn ions and their coupling with the Cu ions. Since these parameters are expected to be doping independent (or weakly dependent), they were found by fitting for the sample $x = 0.01$ and then were kept constant for other concentrations leaving the only free parameter the energy gap Δ.

The results of the fit are shown in Fig. 2(a,b). For the bipolaron formation energy we obtained $\Delta = 460(50)$ K, which is practically doping-independent. This value agrees very well with the value of Δ obtained from the analysis of inelastic neutron-scattering and Raman data in cuprate superconductors [14]. Recently Kochelaev *et al*. performed theoretical calculations of the polaron interactions via the phonon field using the extended Hubbard model [13]. They estimated the bipolaron formation energy and obtained values of 100 K < Δ < 730 K, depending on the value of the Coulomb repulsion between holes on neighboring copper and oxygen sites V_{pd}, $0 < V_{pd} < 1.2$ eV. This means that the experimental value of Δ can be understood in terms of the elastic interactions between the polarons.

It is interesting to compare our results with other experiments performed in lightly doped LSCO. Recently Ando *et al*. measured the in-plane anisotropy of the resistivity ρ_b/ρ_a in single crystals of LSCO with $x = 0.02$-0.04 [4]. They found that at high temperatures the anisotropy is small, which is consistent with the weak orthorhombicity present. However, ρ_b/ρ_a grows rapidly with decreasing temperature below ~ 150 K. This provides macroscopic evidence that electrons self-organize into an anisotropic state because there is no other external source to cause the in-plane anisotropy in $La_{2-x}Sr_xCuO_4$. We notice that the temperature dependence of the narrow EPR line intensity is very similar to that of ρ_b/ρ_a obtained by Ando *et al*. (see Fig. 2(d) in Ref. 4). To make this similarity clear, we plotted I_{narrow}(T) and $\rho_b/\rho_a(T)$ on the same graph (see Fig. 4). It is remarkable that both quantities show very similar temperature dependences. It means that our *microscopic* EPR measurements and the *macroscopic* resistivity measurements by Ando *et al*. provide evidence of the same phenomenon: the formation of hole-rich metallic stripes in lightly doped LSCO well below $x_{\text{cr}} = 0.06$. This conclusion is also supported by a recent angle-resolved photoemission (ARPES) study of LSCO which clearly demonstrated that the metallic quasiparticles exist near the nodal direction below x = 0.06 [16].

A number of experiments on HTSC suggest the possible existence of two quasiparticles: a heavy polaron and a light fermion [15]. In the context of the two-carrier paradigm, the narrow line in the EPR spectra may be attributed to centers with nearly undistorted environment in regions where carriers are highly mobile, whereas the broad line is due to the centers with a distorted environment and slow polaronic carriers. Recent high-resolution ARPES experiments by Lanzara *et al*. clearly showed a kink in the quasiparticle energy versus wavevector plots for different HTSC [17]. The kink at an energy of about 70 meV separates the dispersion into a high-energy part (that is, further from the Fermi energy) and a low-energy part (that is, closer to the Fermi energy) with different slopes. The two different group velocities above and below the kink are probably due to two quasiparticles with different effective masses. In this case a low-energy part of the dispersion would correspond to our narrow EPR line and the high-energy part to broad EPR line. This assumption is strongly supported by very recent isotope effect ARPES experiments by Lanzara *et al*. [18]. They observed that the high-energy quasiparticles have a strong isotope effect, while the low-energy quasiparticles show practically no isotope effect. This is in direct correspondence with our EPR results where the broad EPR line due to heavy polaronic quasiparticles shows a huge isotope effect, whereas the narrow line stemming from metallic regions has no isotope effect. Moreover, looking at Figs. 2,3 one can see that the intensity and linewidth of the narrow line is practically doping independent, while

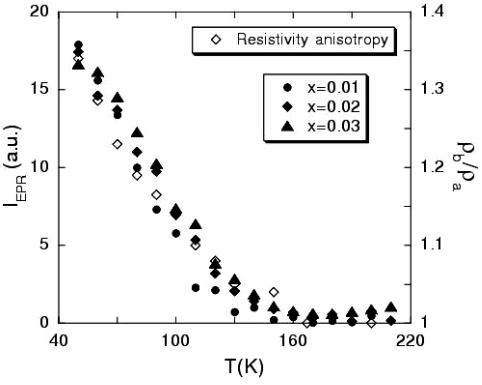

Fig. 4. Temperature dependence of the narrow EPR line intensities in $La_{2-x}Sr_xCu_{0.98}Mn_{0.02}O_4$ and of the resistivity anisotropy ratio in $La_{1.97}Sr_{0.03}CuO_4$ obtained in Ref. 4

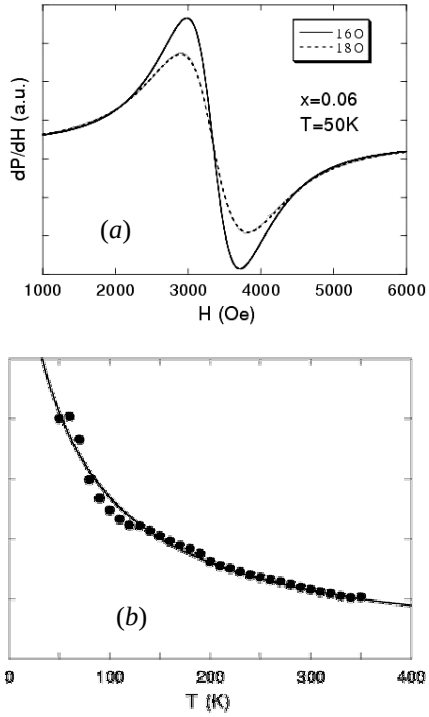

Fig. 5. ***(a)*** *EPR signal of ^{16}O and ^{18}O samples of $La_{1.94}Sr_{0.06}Cu_{0.98}Mn_{0.02}O_4$ measured at T = 50 K under identical experimental conditions. The solid and dashed lines represent the best fits using a single Lorentzian;* ***(b)*** *Temperature dependence of the EPR signal intensity in of $La_{1.94}Sr_{0.06}Cu_{0.98}Mn_{0.02}O_4$. The solid line represents the fit using the Curie-Weiss temperature dependence with the Curie-Weiss temperature θ =40 K*

both the intensity and linewidth of broad line change strongly with the doping. This shows that the local electronic properties of the metallic regions which appear due to the microscopic phase separation and yeld the narrow EPR line are the same in different samples despite different doping levels. This is again in excellent agreement with the ARPES data showing that the Fermi velocity of low-energy quasiparticles are independent of doping in different cuprate families, while the high-energy velocity varies strongly with doping [19]. Also, transport measurements showed that the mobility of charge carriers in LSCO at moderate temperatures remains the same throughout a wide doping range from the lightly-doped AF to optimally doped superconducting regime [20]. These results suggest that the electronic transport is governed by essentially the same mechanism from lightly doped to optimally doped range.

Figs. 5 (a, b) show the EPR spectra and intensity for the $x = 0.06$ sample. It is seen that in contrast to the $x < 0.06$ samples at $x = 0.06$ only a single EPR line is observed and the temperature dependence of the signal intensity recovers an usual Curie-Weiss behavior. On the other hand there is still a substantial isotope effect on the EPR line. To understand the change of the EPR spectra at x = 0.06, one should first comment on the observability of the phase separation in our EPR experiments. The main difference of the EPR signals from the hole-rich and hole-poor regions is the spin relaxation rate of the Cu spin system, which results in different EPR linewidths. One would expect these local differences of the relaxation rate to be averaged out by the spin diffusion. The spin diffusion in the CuO_2 plane is expected to be very fast because of the huge exchange integral between the Cu ions. A rough estimate shows that during the Larmor period a local spin temperature can be transported over 100 Cu-Cu distances. It means that all the different nanoscale regions will relax to the lattice with a single relaxation rate, and we cannot distinguish them with EPR. However, the AF order which appears below T_N in the hole-poor regions in lightly doped LSCO freezes the process of spin diffusion, and this is the reason we can see different EPR lines from the two types of regions. From this we expect that with increasing doping, where magnetic order gets suppressed, spin diffusion will become faster, extended, and we can no longer distinguish different regions with EPR. This is most probably what happens in samples with $x > 0.06$, where only a single EPR line is observed [8]. This does not mean that the phase separation in hole-rich and hole-poor regions does not exist at $x > 0.06$, but that the spin diffusion averages out the EPR response from these regions. In fact, ARPES measurements showed the presence of two quasiparticles in the whole doping range [17,19], indicating that the electronic phase separation exists also at higher doping levels. Also, recent Raman and infrared measurements provided evidence of one-dimensional conductivity in LSCO with $x = 0.10$ [21].

In summary, EPR measurements in lightly doped LSCO revealed the presense of two resonance signals: a narrow and a broad one. Their behavior indicates that the narrow signal is due to hole-rich metallic regions and the broad signal due to hole-poor AF regions. The narrow-line intensity is small at high temperatures and increases exponentially below ~ 150 K. The activation energy inferred, $\Delta = 460(50)$ K, is nearly the same as that deduced from other experiments for the formation of bipolarons, pointing to the origin of the metallic stripes present. We found a remarkable similarity between the temperature dependences of the narrow-line intensity and recently measured resistivity anisotropy in CuO_2 planes in lightly doped LSCO [4]. The results obtained provide the first magnetic resonance evidence of the formation of hole-rich metallic domains in lightly doped LSCO well below $x_{c1} = 0.06$. These results also lend support to the recently proposed model of phase coherence by percolation (PSP) [22]. According to the PSP model the macroscopic phase coherence in superconducting cuprates is determined by random percolation between mesoscopic bipolarons, stripes or clusters. This simple model allows to quantitatively predict the critical carrier concentration for the occurence of the superconductivity as well as to estimate T_c from experimentally measured values of the pairing energy.

This work is supported by SNSF under the grant 7IP062595, AS are partially supported by INTAS-01-0654 and CRDF REC-007.

References

1. J.G. Bednorz and K.A. Müller, Z. Phys. B **64**, 189 (1986).
2. See, for instance, *Phase separation in Cuprate Superconductors*, edited by K.A. Müller and G. Benedek (World Scientific, Singapore, 1993).
3. J.H. Cho *et al*., Phys. Rev. Lett. **70**, 222 (1993).

4. Y. Ando *et al*., Phys. Rev. Lett. **88**, 137005 (2002).
5. A.N. Lavrov, S. Komiya and Y. Ando, Nature **418**, 385 (2002).
6. V.J. Emery and S.A. Kivelson *et al*., Physica C **209**, 597 (1993).
7. T. Imai *et al*., Phys. Rev. Lett. **70**, 1002 (1993).
8. A. Shengelaya *et al*., Phys. Rev. B **63**, 144513 (2001).
9. B.I. Kochelaev *et al*., Phys. Rev. B **49**, 13106 (1994).
10. Ch. Niedermayer *et al*., Phys. Rev. Lett. **80**, 3843 (1998).
11. L.K. Aminov and B. I. Kochelaev, Zh. Eksp. Theor. Fiz. **42**, 1303 (1962).
12. R. Orbach and M. Tachiki, Phys. Rev. **158**, 524 (1967).
13. B.I. Kochelaev *et al*., Mod. Phys. Lett. B **17**, 415 (2003).
14. V.V. Kabanov and D. Mihailovic, Phys. Rev. B **65**, 212508 (2002).
15. D. Mihailovic and K. A. Müller, in *High-Tc Superconductivity: Ten Years After the Discovery*, E. Kaldis *et al*., eds. Kluwer Academic Publishers (1997) p. 243.
16. T. Yoshida *et al*., Phys. Rev. Lett. **91**, 027001 (2003).
17. A. Lanzara *et al*., Nature **412**, 510 (2001).
18. A. Lanzara *et al*., unpublished.
19. X. J. Zhou *et al*., Nature **423**, 398 (2003).
20. Y. Ando *et al*., Phys. Rev. Lett. **87**, 017001 (2001).
21. F. Venturini *et al*., Phys. Rev. B **66**, R060502 (2002).
22. D. Mihailovic *et al*., Europhys. Lett. **57**, 254 (2002).